EFFECT OF SURFACE MICROMORPHOLOGY AND HYDROPHOBICITY ON CONDENSATION EFFICIENCY OF DROPLETS USING THE LATTICE BOLTZMANN METHOD

by

Lijun LIU [a,b]***, Gaojie LIANG*** [b*]***, Haiqian ZHAO*** [b*]***, and Xiaoyan LIU*** [b]

[a] School of Electronic and Information Engineering, Changshu Institute of Technology, Changshu, Jiangsu, China
[b] School of Civil Engineering and Architecture, Northeast Petroleum University, Daqing, Heilongjiang, China

Original scientific paper
https://doi.org/10.2298/TSCI210506287L

In the present study, the effects of the surface morphology and surface hydrophobicity on droplet dynamics and condensation efficiency are investigated using the lattice Boltzmann method. Different surface morphologies may have different condensation heat transfer efficiencies, resulting in diverse condensation rates under the same conditions. The obtained results show that among the studied morphologies, the highest condensation rate can be achieved for conical micro-structures followed by the triangle micro-structure, and the columnar micro-structure has the lowest condensation rate. Moreover, it is found that when the surface micro-structure spacing is smaller and the surface micro-structure is denser, the condensation heat transfer between the surface structure and water vapor facilitates, thereby increasing the condensation efficiency of droplets. Furthermore, the condensation process of droplets is associated with the surface hydrophobicity. The more hydrophobic the surface, the more difficult the condensation heat transfer and the longer the required time for droplet nucleation. Meanwhile, a more hydrophobic surface means that it is harder for droplets to gather and merge, and the corresponding droplet condensation rate is also lower.

Key words: *lattice Boltzmann method, droplet, micro-structure, condensation rate*

Introduction

Studies show that dropwise condensation has a higher heat transfer coefficient than film condensation so that it is widely applied in diverse applications, including steam power generation, seawater desalination, thermal power plant, petrochemical plants, and other industrial applications [1, 2]. With the increasing escalation of the energy crisis, dropwise condensation heat transfer technology has attracted many scholars in recent years [3]. The performed investigations show that the vapor-solid contact surface can significantly improve the condensation phase transformation efficiency in the vapor-liquid phase transformation process. Therefore, it is of great significance to study the movement of droplets on the micro-structure surface and the condensation heat transfer mechanism.

Recently, researchers have carried numerous experiments about the influence of droplet condensation on the heat transfer and dynamic characteristics of the droplet condensation,

[*] Corresponding authors, e-mails: a1062378608@163.com; dqzhaohaiqian@163.com

mainly focusing on the effects of surface wettability [4, 5], surface morphology [6, 7] and subcooling [8, 9]. Xie *et al.* [10] carried out dropwise condensation experiments on different surfaces and found that the wettability of superhydrophobic surfaces decreases as the temperature increases, while the smooth hydrophobic surfaces could maintain stable heat transfer. Chen *et al.* [11] found that surface roughness significantly affects the number and frequency of the droplet jump. However, the specific effect of the surface micro-structure on the droplet condensation heat transfer efficiency is still unclear.

It should be indicated that simulating the droplet condensation in the microscopic state is an enormous challenge for numerical methods. The conventional CFD method can hardly quantify the interface transfer of mass and heat [12]. It is worth noting that high computational costs and low efficiency limit the application of molecular dynamics in this area [13]. In the past two decades, lattive Boltzmann method (LBM) has developed into an effective method widely used to simulate multi-phase flows and phase change processes [14, 15]. Studies show that the surface micro-structure plays an important role in enhancing condensation heat transfer and condensation kinetics [16, 17]. Therefore, numerous investigations have been carried out on the condensation heat transfer of droplets with the surface morphology as the object. Moreover, the effects of different morphologies such as columnar [18], triangle [19], on strengthening the condensation heat transfer of droplets have been studied. In this regard, Zhang *et al.* [20] studied the droplet condensation kinetics on the superhydrophobic surfaces and found that the density of the surface micro-structure has an important influence on the droplet condensation efficiency. Recently, condensation heat transfer research on the surface wettability has become a research hotspot [21, 22]. Li *et al.* [23] simulated the droplet condensation on different hydrophobic surfaces using a phase transition model. The results show that the condensation efficiency on a hydrophilic surface is higher than that on a hydrophobic surface.

However, the majority of studies in the field of the surface micro-morphology, hydrophobicity and the droplet condensation heat transfer have focused on the influence of a single influencing factor on the droplet condensation process in isolation, ignoring the influence of multiple factors on droplet condensation kinetics. The real condensation process is the result of the interaction between various influencing factors. It should be indicated that a comprehensive study on the influence of the surface morphology and hydrophobicity on droplet condensation can result in a conclusion closest to the real condensation process, which has guiding significance for strengthening the condensation heat transfer process of droplets on the hydrophobic surface.

In the present study, the multi-component multi-phase SC model [24] is used to simulate the droplet condensation on the micro-structure surface. In the simulation process, the effects of different surface micro-structures, including columnar surface, triangle surface and conical surface, and micro-structure spacing and hydrophobicity on the condensation quality and efficiency of droplets are comprehensively considered. The main objective of this article is to reveal the influence of the surface micro-structures and wettability on the condensation and growth of droplets.

Simulation method

In this study, the BGK collision operator used in pseudo-potential models is adopted commonly, and the two-dimension, nine-velocity (D2Q9) model is used to simulate the density distribution in the process of water vapor condensation. The density distribution formula describing the evolution of particles is expressed [20]:

$$f_i^\lambda\left(x+e_i\delta t,t+\delta t\right)-f_i^\lambda\left(x,t\right)=-\frac{1}{\tau^\lambda}\left[f_i^\lambda\left(x,t\right)-f_i^{\lambda(\mathrm{eq})}\left(x,t\right)\right] \tag{1}$$

where $f_i^\lambda(x, t)$ is the density distribution function of the λ^{th} component in the i^{th} velocity direction, τ^λ stands for relaxation time, and the relation between it and viscosity coefficient is $\nu^\lambda = c_s^2(\tau^\lambda - 0.5)\delta t$. The equilibrium distribution function:

$$f_i^{\lambda(\mathrm{eq})}\left(x\right)=\omega_i\rho^\lambda(x,t)\left[1+\frac{3[e_iu^\lambda(x,t)]}{c_s^2}+\frac{4.5[e_iu^\lambda(x,t)]^2}{c_s^4}-\frac{1.5[u^\lambda(x,t)]^2}{2c_s^2}\right] \tag{2}$$

where u^λ represents the macroscopic velocity of the fluid, ρ^λ represents the density of the fluid of different components, ω_i represents the weight coefficient, and e_i represents the discrete velocity, which provided:

$$\omega_i=\begin{cases}\dfrac{4}{9}, & i=0\\[2mm] \dfrac{1}{9}, & i=1\sim 4\\[2mm] \dfrac{1}{9}, & i=5\sim 8\end{cases} \tag{3}$$

$$e_i=\begin{cases}\left(0,0\right), & i=0\\ (\pm1,0),\ (0,\pm1), & i=1\sim 4\\ (\pm1,\pm1), & i=5\sim 8\end{cases} \tag{4}$$

The density and macroscopic velocity of fluid can be expressed:

$$\rho^\lambda=\sum_{i=0}^{8}f_i \tag{5}$$

$$u^\lambda\left(x,t\right)=u'\left(x,t\right)+\frac{\tau^\lambda\delta tF^\lambda(x,t)}{\rho^\lambda} \tag{6}$$

where F^λ is the force acting on the λ^{th} component, which includes the interaction between different fluids $F_{\mathrm{in}}^\lambda(x,t)$ and the interaction between fluid and solid wall $F_{\mathrm{ads}}^\lambda(x,t)$:

$$F^\lambda=F_{\mathrm{in}}^\lambda(x)+F_{\mathrm{ads}}^\lambda(x) \tag{7}$$

The interaction force between fluids of different components can be indicated:

$$F_{\mathrm{in}}^\lambda(x,t)=-\psi^\lambda(x,t)\sum G(x,x')\sum_{i=0}^{8}\psi^{\bar\lambda}(x',t)e_i \tag{8}$$

where λ and $\bar\lambda$ indicate two different fluid components, $\psi^\lambda(x, t)$ and $\psi'(x', t)$ as effective densities can be expressed [25]:

$$\psi^\lambda(x,t)=\rho^\lambda(x,t) \tag{9}$$

$$\psi^{\bar\lambda}(x,t)=\rho^{\bar\lambda}(x,t) \tag{10}$$

The pressure value at position x is determined:

$$P(x,t)=\frac{\sum_\lambda\rho^\lambda(x,t)}{3}+\frac{G}{3}\psi^\lambda(x,t)\psi^{\bar\lambda}(x,t) \tag{11}$$

The interaction force between fluid and solid is expressed:

$$F_{\text{ads}}^{\lambda}(x,t) = -\rho^{\lambda}\left(x,t\right)\sum_{i=0}^{8}\omega_i G_{\text{ads}}^{\lambda} s(x+e_i\delta t) \tag{12}$$

where s is the wall index. When the lattice is solid or liquid, its values are 1 or 0, respectively. The strength of the wall force of fluid and solid is controlled by G^k_{ads}. Therefore, the droplet contact angle can be controlled by controlling the size of G^k_{ads}. In this work, the model system includes two-components: water vapor and non-condensing gases [20]. The relationship between G^1_{ads} (H_2O/solid) and G^2_{ads} (non-H_2O/solid) is $G^1_{\text{ads}} = -G^2_{\text{ads}}$.

Results and discussions

Model validation

Firstly, the correctness of the aforementioned model is verified by verifying the Laplace law. The pressure difference inside and outside the droplet is proportional to the reciprocal of the droplet radius according to the Laplace law, which can be expressed:

$$\Delta p = \frac{\sigma}{r} \tag{13}$$

where Δp is the pressure difference between inside and outside the droplet and σ represents the surface tension of the droplet. The simulation calculation locale is set to 101×101 lattice unit (lu) and the center of the droplet is set in the center of the calculation region (50, 50). Periodic boundary conditions is applied to the surrounding boundaries of the calculation region and neglect the effect of gravity. The radius of droplet is taken as 14 lu, 15 lu, 17 lu, 20 lu, 22 lu, 25 lu, and 28 lu, respectively. The variation of the internal and external pressure difference of the droplet with the reciprocal of the droplet radius is recorded after the droplet state remained stable. It is found that Δp and $1/r$ have a linear fitting relationship through the analysis of each data point, as shown in fig. 1(a), which is consistent with previous report [26]. The slope of the fitting line is the surface tension of the droplet which is calculated to be about 0.2763.

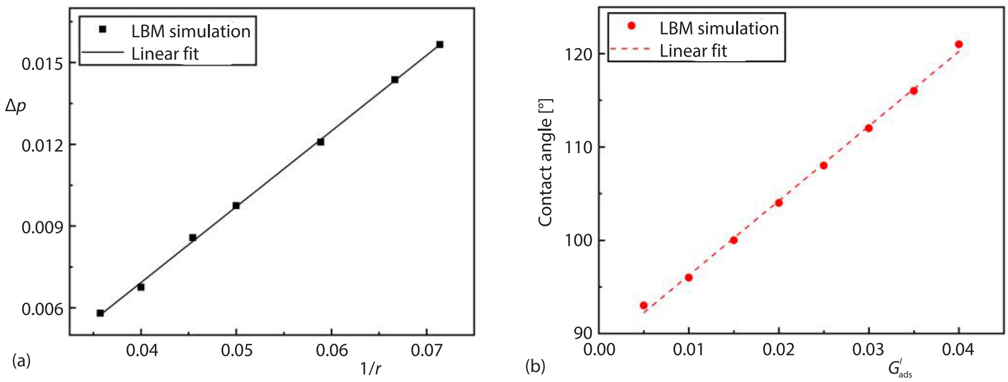

Figure 1. Model verification; (a) relationship between the pressure difference inside and outside the droplet and the reciprocal of droplet radius and (b) relationship between contact angle and solid-liquid contact coefficient G^1_{ads}

The contact angle can be verified by adjusting G^k_{ads} in the SC model. Similarly, set the calculation area to 101×101 lu, the left and right boundaries are set as periodic boundary and standard bounce-back boundary is adopted at the upper and bottom boundaries. The droplet with a radius of 14 lu is lay at the bottom, then adjust the intensity coefficient G^1_{ads}. The contact angle between the droplet and the solid surface is recorded after the droplet state remained stable. The linear relationship between contact angle and G^{1}_{ads} as shown in figure 1(b), which is consistent with previous studies [27, 28].

System parameters and boundary conditions

The computational region is set at 211×101 lu in this study as shown in fig. 3. The initial density parameters of water vapor (H_2O) and non-condensable gases (non-H_2O) in the calculation area are saver as ρ_{H_2O} = 0.035 mu·lu^{-2} (mass units per square lattice unit) and $\rho_{non\text{-}H_2O}$ = 0.965 mu·lu^{-2}. Standard bounce-back boundary scheme is employed at the bottom boundary and the left and right boundaries are set as periodic boundary. Zou [29] pressure boundary is adopted at the upper boundary to provide water vapor to the system continuously. The gases densities at the inlet of the upper boundary are remained at ρ_{H_2O} = 0.08 mu·lu^{-2} and $\rho_{non\text{-}H_2O}$ = 0.92 mu·lu^{-2}. As shown in the enlarged figure on the right side of fig. 2, the bottom structure of the system adopts columnar micro-structure, conical micro-structure and triangle micro-structure. The letters W, D, H, and F symbolizes the base width, spacing, height and top width of the micro-structure, respectively, [30].

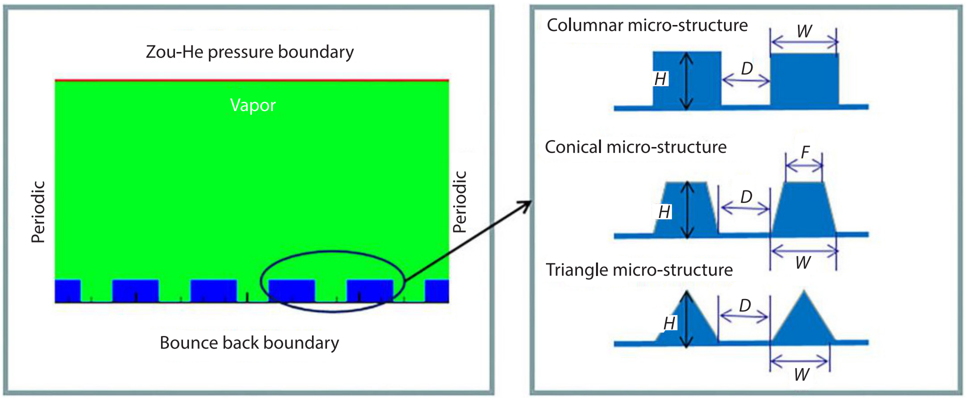

Figure 2. Model and simulation parameters

Effect of surface micromorphology on droplet condensation

Effect of different morphologies on droplet condensation

Studies show that the surface morphology has a significant effect on the condensation heat transfer of droplets [27]. Accordingly, three types of the surface micro-structures, including the triangle micro-structure, conical micro-structure and columnar micro-structure, are designed to simulate the condensation heat transfer of droplets. Figure 3 shows these micro-structures. The size of the simulation area is 211×101 lu, and the geometric size of the micro-structure is set to W = 20 lu, F = 10 lu, D = 15 lu, and H = 10 lu. Boundary conditions will be discussed in section *System parameters and boundary conditions*. In fig. 3, the color change in the diagram represents the density change of water vapor, the change in the density of water vapor from 0.05-0.9 indicates that the water vapor condenses into droplets. Figure 3 illustrates that the water vapor begins to accumulate on the micro-structure surface after the simulation. When t = 5000, the droplet nucleation appears on the triangle and conical micro-structure surfaces, while no droplet nucleation occurs on the columnar micro-structure surface. Meanwhile, the nucleation droplet on the triangle surface is significantly larger than that on the conical micro-structure surface. It is found that under the same condensation conditions, the triangle surface has the shortest nucleation time, while the columnar surface has the lowest nucleation time and the nucleation time of the conical micro-structure surface is in the middle. At $t = 15000$, the droplets on the triangle micro-structure surface coalescence, while the droplets on other surfaces still exist in a single form. Then, the droplets absorb the water vapor in the surrounding liquid phase and continue to grow. At $t = 22000$, it is observed that the droplet radius generated on the triangle and conical micro-structure surface is significantly larger than that on the columnar micro-structure surface. It is concluded that the droplet condensation efficiency on the triangle and conical micro-structure surfaces is greater than that on the columnar micro-structure surface.

In order to confirm the condensation efficiency of droplets on different types of micro-structure surfaces, distributions of the condensation mass and condensation rate on different types of micro-structure surfaces over time are compared. It is observed that the surface morphology significantly affects the condensation quality and condensation efficiency of droplets. Figure 4(a) illustrates that the condensation mass and condensation velocity of the columnar micro-structure surface are lower than those of the other micro-structure surfaces at the same time step. Moreover, it is found that the upward trend of the condensation mass curve on the surface of the triangle structure is relatively smooth and uniform, that on the surface of the conical micro-structure is relatively rapid. Before $t = 15000$, the condensation mass of droplets on the triangle micro-structure surface is larger than that on the conical micro-structure surface. However, after $t = 15000$, the condensation mass of droplets on the conical micro-structure surface exceeds that on the triangle micro-structure surface, and the gap widens as time progresses. Compared with the condensation velocity curve in fig. 4(b), it is observed that the condensation velocity of droplets on the conical micro-structure surface increases continuously, while the condensation velocity on the triangle micro-structure surface remains in a relatively stable state. Although the condensation velocity on the columnar micro-structure surface increases, the increment is extremely limited.

Figures 3 and 4 reveal that under the same simulation conditions, the condensation efficiency of studied micro-structures in an ascending order includes the columnar micro-structure surface, triangle micro-structure surface and the conical micro-structure surface. Accordingly, the conical micro-structure is utilized to investigate the influence of the surface topography geometric parameters on the condensation efficiency of droplets.

Effect of surface morphology spacing on droplet condensation

The spacing of the surface micro-structure has a significant influence on the dropwise condensation heat transfer. Therefore, the conical micro-structure surfaces with different spacing are simulated in this study. Figure 5 shows the simulation results of the condensation process on the surface of the conical micro-structure with different spacing. Except for the structural spacing D, the size of the simulation area is 211×101 lu and the geometric size parameters of the conical micro-structure are consistent with those mentioned in section *Effect of different morphologies on droplet condensation*. Figures 5(a)-5(c) show that the spacing of conical micro-structures is $D = 22$, 15, and 10, respectively. It is observed that the condensation process of droplets on the conical micro-structure surface is similar to that shown in fig. 3(b). Water vapor initially gathers at the bottom of the conical micro-structure surface, then nucleates at the top of the conical micro-structure and absorbs water molecules in the surrounding liquid phase. Moreover, it is found that the nucleation time of droplets on the micro-structure surface with different spacing is roughly the same, indicating that the spacing of the surface micro-structure does not affect the overall trend of the droplet condensation.

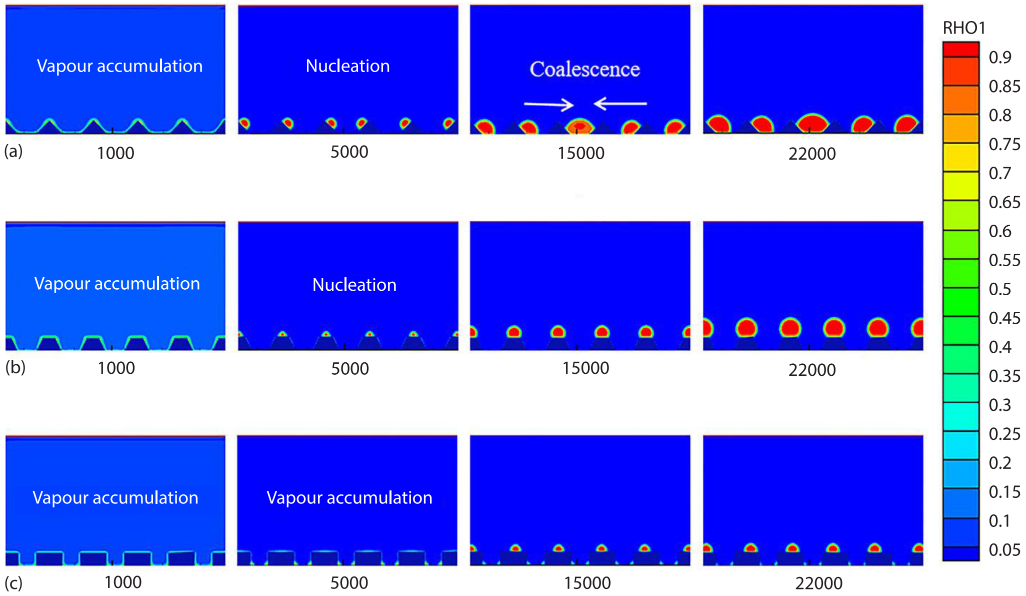

Figure 3. Condensation process of droplets on different types of bottom micromorphology; (a) triangle micro-structure, (b) conical micro-structure, and (c) columnar micro-structure

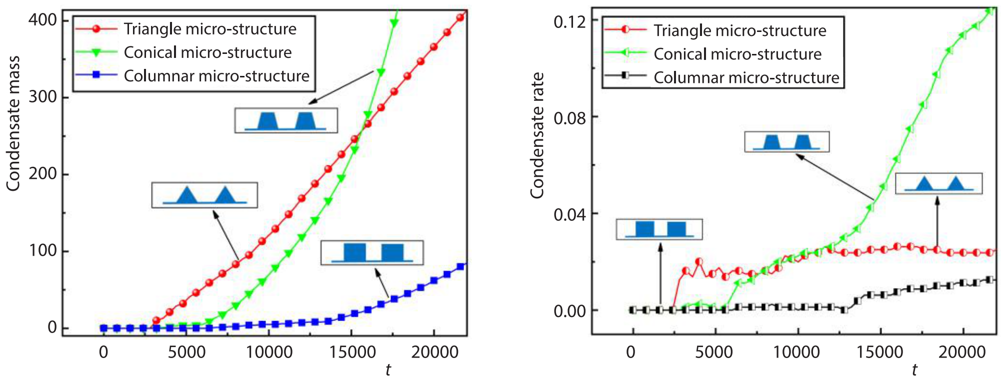

Figure 4. Condensation mass and rate diagrams of droplets with different morphologies; (a) the relationship between condensation mass and time step *t* and (b) the relationship between condensation rate and time step *t*

In this section, the effect of the micro-structure spacing on the condensation heat transfer performance of droplets is investigated. Figure 6 illustrates the variations of the condensation mass and condensation rate at the same time steps on the surface of three conical micro-structures with different spacing. It is found that at the initial stage of the condensation, the surface structure spacing has a negligible impact on the condensation quality and condensation rate of droplets. However, as the condensation process progresses, the difference in the condensation quality of droplets on the surface of different spacing micro-structures increases. Figure 6(b) presents the variation of the condensation rate against time, which shows the condensation rate of droplets. Accordingly, it is found that the micro-structure surface with a smaller spacing size has a faster condensation rate.

Figures 5 and 6 show that under the same condensation conditions, the smaller the distance between surface micro-structures, the faster the condensation rate of droplets, and the higher the condensation heat transfer efficiency of droplets.

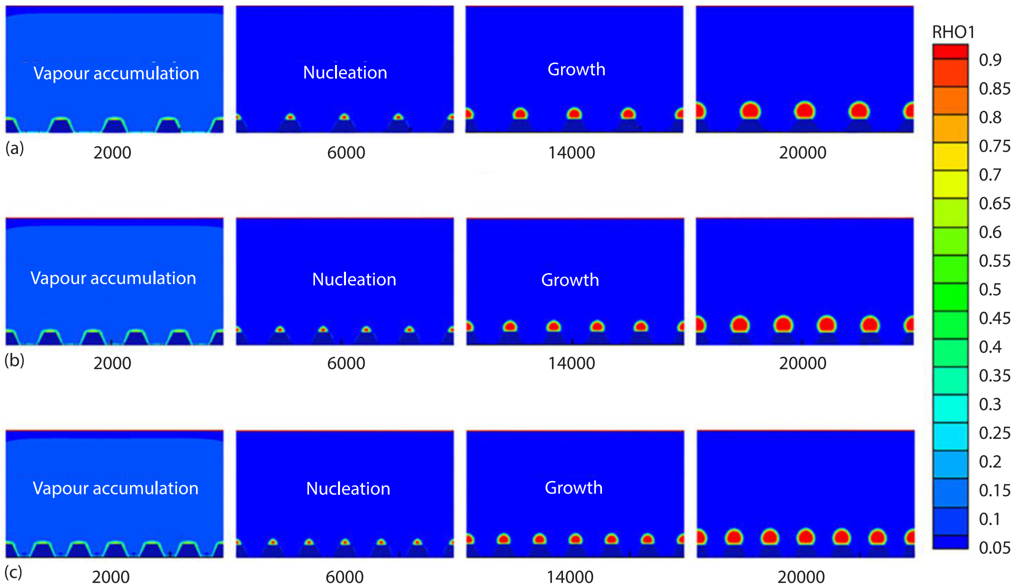

Figure 5. Condensation process of droplets on the same type and different spacing bottom microtopography; (a) *D* = 22 lu, (b) *D* = 15 lu, and (c) *D* = 10 lu

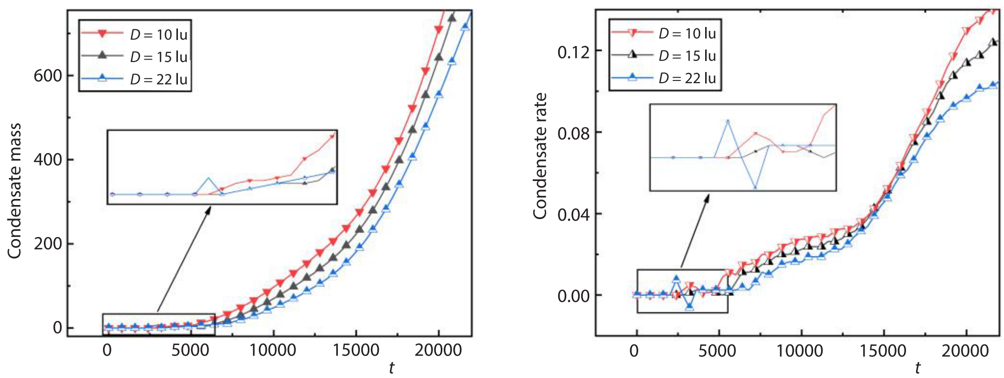

Figure 6. Condensation mass and rate diagrams of droplets at different spacing bottom microtopography; (a) the relationship between condensation mass and time step *t* and (b) the relationship between condensation rate and time step *t*

Effect of surface hydrophobic on droplet condensation

Figure 7 shows the condensation evolution of droplets on the micro-structure surface with different hydrophobicities, including $G^1_{ads} = 0.02$, $G^1_{ads} = 0.03$, and $G^1_{ads} = 0.04$. It should be indicated that the size of the simulated region is 211×101 lu, and the geometric parameters of the conical micro-structure are $W = 20$ lu, $F = 10$ lu, $D = 10$ lu, and $H = 10$ lu. The remaining boundary conditions were discussed in section *System pa-*

rameters and boundary conditions. It is observed that when t = 4000, the droplet nucleation occurs on the top of the conical micro-structure with G^1_{ads} = 0.02. However, only water vapor accumulation occurs on the surface of the micro-structure with G^1_{ads} = 0.03 and G^1_{ads} = 0.04. When t = 5000, the droplet nucleation appears on the micro-structure surface with G^1_{ads} = 0.03, and the droplet nucleation time on the micro-structure surface with G^1_{ads} = 0.04 occurs at t = 7000. Then water molecules grow in the droplet absorption system on three distinct hydrophobic surfaces. At t = 30000, the droplets in fig. 7(a) coalescence due to the continuous growth breaking through the limitation of the surface spacing of the micro-structure. It is worth noting that the droplets in figs. 7(b) and 7(c) are still in a single form.

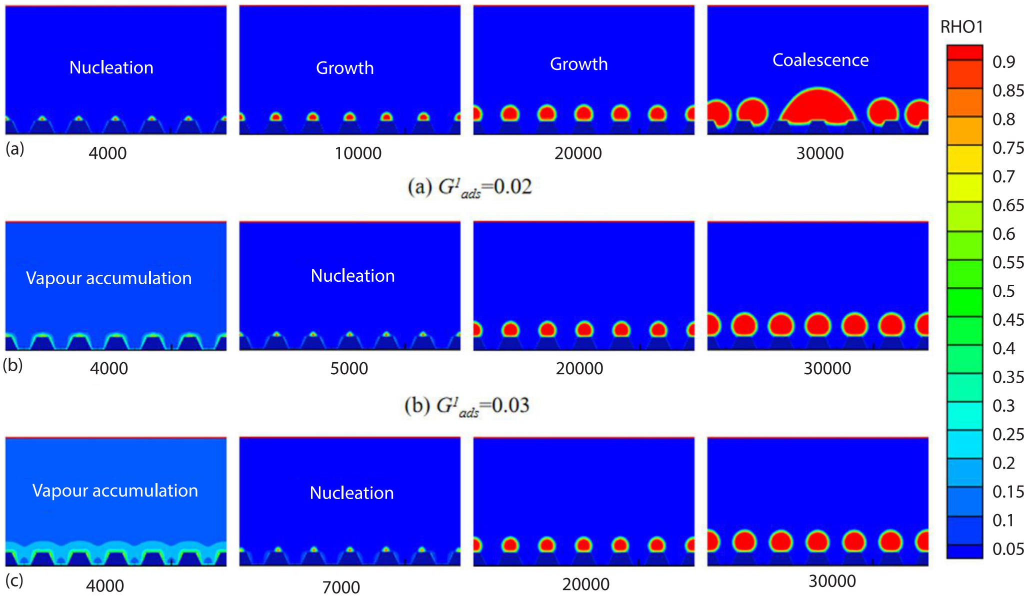

Figure 7. Condensation process of droplets on different hydrophobic surface; (a) G^1_{ads} = 0.02, (b) G^1_{ads} = 0.03, and (c) G^1_{ads} = 0.04

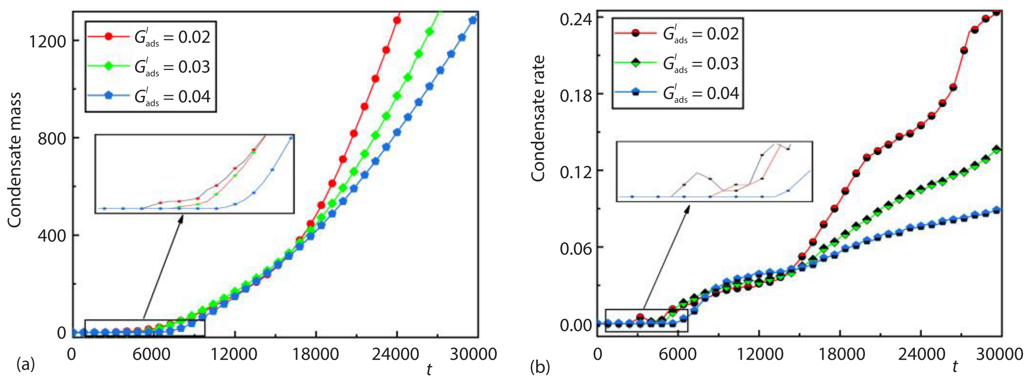

Figure 8. Condensation mass and rate of droplets on different hydrophobic surfaces; (a) the relationship between condensation mass and time step *t* and (b) the relationship between condensation rate and time step *t*

Moreover, the effect of the surface hydrophobicity on the condensation heat transfer performance of droplets is investigated. Figure 8 shows the distribution of the condensation mass and condensation rate of droplets with three surface hydrophobicity conical micro-structures over time. Figure 8(a) shows that the more hydrophobic the surface, the later the condensation mass begins to increase. Moreover, fig. 8(b) reveals that condensation rates of droplets on the micro-structure surface with different hydrophobicity are very different, and the condensation rate of droplets on the surface with stronger hydrophobicity is smaller. Furthermore, it is observed that the condensation kinetic behavior of droplets also affects the condensation rate of droplets. For instance, the rapid increment in the condensation rate of surface droplets with $G^1_{\rm ads} = 0.02$ in fig. 8(b) mainly originates from the coalescence of droplets.

Figures 7 and 8 indicate that the condensation efficiency of droplets is also correlated to the surface hydrophobicity. The stronger the hydrophobicity, $G^1_{\rm ads}$, the more difficult the nucleation and growth of droplets. Moreover, the longer the waiting time for the nucleation, the lower the overall condensation efficiency.

Conclusions

In the present study, a 2-D multi-component and multi-phase flow LBM model is proposed to simulate the condensation of droplets on the micro-structure hydrophobic surface. Moreover, the influence of the surface micro-structure and hydrophobicity on the growth and condensation efficiency of condensation droplets is investigated. Based on the obtained results, the following conclusions are as follows.

- The condensation efficiency of the droplet is correlated to the type of the surface micromorphology. The condensation efficiency of the studied surfaces in descending order are the conical surface, the triangle surface, and the column surface.
- The condensation efficiency of the droplet is correlated to the geometric parameters of the surface micro-structure. The smaller the distance between the surface micro-structure, the faster the condensation rate of the droplet and the higher the condensation efficiency of the surface.
- The condensation process of droplets is linked to the surface hydrophobicity. The higher the surface hydrophobicity, the longer the nucleation time of droplets, and the lower the corresponding condensation efficiency.

Acknowledgment

This work is supported by the Nature Science Foundation of Heilongjiang Province(YQ2019E008 and LH2020E017), Education Department Project of Heilongjiang Province (2018GPQZ09), and Outstanding Youth Reserve Program of Northeast Petroleum University(SJQHB202003)

References

[1] Khawaji, A. D., *et al*., Advances in Seawater Desalination Technologies, *Desalination*, 221 (2008), 3, pp. 47-69
[2] Boreyko, J. B., *et al.*, Vapor Chambers with Jumping-Drop Liquid Return from Superhydrophobic Condensers, *International Journal of Heat & Mass Transfer*, *61* (2013), 6, pp. 409-418
[3] Rose, J. W., Dropwise Condensation Theory and Experiment: A Review, Proc. Imeche – Part A2: *Journal Power & Energy*, *216* (2005), 2, pp. 115-128
[4] Zhang, K., *et al*., Ratio Dependence of Contact Angle for Droplet Wetting on Chemically Heterogeneous Substrates, *Colloids & Surfaces A Physicochemical & Engineering Aspects*, *539* (2017), 3, pp. 237-242
[5] Pan, B., *et al*., Wetting Dynamics of Nanoliter Water Droplets in Nanoporous Media, *Journal of Colloid and Interface Science*, *589* (2020), May, pp. 411-423

[6] Jung, Y. C., *et al*., Wetting Behaviour during Evaporation and Condensation of Water Microdroplets on Superhydrophobic Patterned Surfaces, *Journal of Microscopy*, *229* (2010), 1, pp. 127-140
[7] Cheng, J., *et al*., Condensation Heat Transfer on Two-Tier Superhydrophobic Surfaces, *Applied Physics Letters*, *101* (2012), 13, 173108
[8] Miljkovic, N., *et al*., Jumping-Droplet Electrostatic Energy Harvesting, *Applied Physics Letters*, *105* (2014), 1, 175
[9] Wen, R., *et al*., Hierarchical Superhydrophobic Surfaces with Micropatterned Nanowire Arrays for High-Efficiency Jumping Droplet Condensation, *Acs Applied Materials & Interfaces*, *9* (2017), 51, pp. 44911-44921
[10] Xie, J., *et al*., Dropwise Condensation on Superhydrophobic Nanostructure Surface – Part I: Long-Term Operation and Nanostructure Failure, *International Journal of Heat and Mass Transfer*, *129* (2018), 6, pp. 86-95
[11] Chen, X., *et al*., Characterization of Coalescence-Induced Droplet Jumping Height on Hierarchical Superhydrophobic Surfaces, *ACS Omega*, *2* (2017), 6, pp. 2883-2890
[12] Sazhin, S.S., *et al.*, Transient Heating of an Evaporating Droplet, *International Journal of Heat & Mass Transfer*, *53* (2010), 14, pp. 2826-2836
[13] Alam, M. S., *et al.*, Comparative Molecular Dynamics Simulations of Homogeneous Condensation of Refrigerants, *International Journal of Thermal Sciences*, *141* (2019), 5, pp. 187-198
[14] Raabe, D., Overview of the Lattice Boltzmann Method for Nanoand Microscale Fluid Dynamics in Materials Science and Engineering, *Modelling Simul. Mater. Sci. Eng*., *12* (2004), 3, pp. 11-15
[15] Varnik, F., *et al*., Stability and Dynamics of Droplets on Patterned Substrates: Insights from Experiments and Lattice Boltzmann Simulations, *Journal of Physic: Condensed Matter*, *23* (2011), 18, 184112
[16] Rui, W., *et al*., Bio-Inspired Superhydrophobic Closely Packed Aligned Nanon-eedle Architectures for Enhancing Condensation Heat Transfer, *Advanced Functional Materials*, *28* (2018), 49, 1800634
[17] Checco, A., *et al*., Robust Superhydrophobicity in Large-Area Nanostructured Surfaces Defined by Block-Copolymer self Assembly, *Advanced Materials*, *26* (2014), 6, pp. 886-891
[18] Peng, B., *et al*., Analysis of Droplet Jumping Phenomenon with Lattice Boltzmann Simulation of Droplet Coalescence, *Applied Physics Letters*, *102* (2013), 15, pp. 1776-1785
[19] Shi, Y., et al., Investigation of Coalesced Droplet Vertical Jumping and Horizontal Moving on Textured Surface Using the Lattice Boltzmann Method, *Computers and Mathematics with Applications*, *75* (2017), 4, pp. 1213-1225
[20] Zhang, Q., *et al.*, Lattice Boltzmann Modelling of Droplet Condensation on Superhydrophobic Nanoarrays, *Langmuir, 30* (2014), 42, pp. 12559-12569
[21] Yu, J., *et al*., Effects of Geometrical Characteristics of Surface Roughness on Droplet Wetting, *The Journal of Chemical Physics*, *127* (2007), 23, pp. 234704-234704
[22] Bo, Z., *et al.*, Spontaneous Wenzel to Cassie Dewetting Transition on Structured Surfaces, *Physical Review Fluids*, *1* (2016), 7, 073904
[23] Li, M., *et al*., Study on Nucleation Position and Wetting State for Dropwise Condensation on Rough Structures with Different Wettability Using Multi-phase Lattice Boltzmann Method, *International Journal of Heat and Mass Transfer*, *131* (2019), 5, pp. 96-100
[24] Shan, X., *et al.*, Lattice Boltzmann Model for Simulating Flows with Multiple Phases and Components, *Phys. Rev. E Stat Phys. Plasmas Fluids Relat Interdiscip Topics*, *47* (1993), 3, pp. 1815-1819
[25] Liang, G., *et al.*, Study on Droplet Nucleation Position and Jumping on Structured Hydrophobic Surface using the Lattice Boltzmann Method, *Thermal Science*, *26* (2022), 1B, pp. 1477-1486
[26] Mazloomi, A., *et al*., Gravity-Driven Thin Liquid Films over Topographical Substrates, *European Physical Journal E*, *36* (2013), 6, 58
[27] Haibo, *et al*., Proposed Approximation for Contact Angles in Shan-and-Chen-type Multicomponent Multi-Phase Lattice Boltzmann Models, *Physical Review E*, *76* (2007), 6, 0666701
[28] Hao, P. F., *et al.*, Wetting Property of Smooth and Textured Hydrophobic Surfaces under Condensation Condition, *Science China*, *57* (2014), 11, pp. 2127-2132
[29] Zou, Q., On Pressure and Velocity Boundary Conditions for the Lattice Boltzmann BGK Model, *Physics of Fluids*, *9* (1996), 6, 1591
[30] Xin, W. A., *et al*., Lattice Boltzmann Simulation of Dropwise Condensation on the Micro-Structured Surfaces with Different Wettability and Morphologies, *International Journal of Thermal Sciences*, *160* (2020), Feb., 106643

Paper submitted: May 6, 2021
Paper revised: July 15, 2021
Paper accepted: July 17 , 2021

© 2022 Society of Thermal Engineers of Serbia
Published by the Vinča Institute of Nuclear Sciences, Belgrade, Serbia.
This is an open access article distributed under the CC BY-NC-ND 4.0 terms and conditions